J Mol Model (2008) 14:343–351
DOI 10.1007/s00894-008-0275-2

ORIGINAL PAPER

Molecular dynamics simulations on hydrogen adsorption in finite single walled carbon nanotube bundles

M. Todd Knippenberg · Steven J. Stuart · Hansong Cheng

Received: 15 September 2007 / Accepted: 21 January 2008 / Published online: 20 February 2008

Abstract Molecular dynamics simulations of the adsorption of hydrogen molecules in finite single-walled carbon nanotube bundles are presented using a curvature dependent force field. The heat of formation and the effective adsorption capacity are expressed as a function of H_2 distance from adsorbent. The heat of adsorption decreases rapidly with the distance and increasing H_2 loading results in weakening adsorption strength. The effects of nanotube packing and bundle thickness on hydrogen adsorption strength were investigated and the results show that the heat of adsorption can be improved slightly if hydrogen molecules are placed in thicker and inhomogeneously packed nanotube bundles. Only very small diameter nanotube bundles were found to hold promise for significant hydrogen storage for onboard applications.

Keywords Hydrogen storage · Molecular dynamics · Single walled carbon nanotubes

Introduction

The storage of hydrogen by adsorption using various new forms of carbon-based materials has recently gained widespread attention as one of the key components of a future hydrogen economy. The emerging use of polymer electrolyte membrane (PEM) fuel cells for stationary power generation and for vehicle applications depends on efficient hydrogen storage. Carbon-based materials are typically lightweight, due to the low atomic mass of carbon, which helps improve gravimetric energy storage density. It has been known for some time that high-surface-area activated carbons reversibly adsorb a considerable amount of hydrogen at cryogenic temperatures [1, 2]. However, this restriction to very low temperatures may offer no practical or economic advantages over the current use of high pressure compressed hydrogen or liquefied hydrogen for hydrogen storage. The discovery of single-walled carbon nanotubes (SWCNTs) has opened the exploration of these materials for the separation and adsorption of gases at near-ambient temperature and moderate pressures. SWCNTs are composed of single graphene sheets (one layer of graphite), rolled into a seamless cylinder with a diameter that generally ranges from 0.7 – 2.0 nm. SWCNTs rarely exist as individual nanotubes but instead are isolated in organized bundles of nanotubes held together by van der Waals interactions. The reported heat of adsorption of H_2 on SWCNTs (−4.7 kcal mol^{-1}) [3, 4] is much higher than in previous measurements involving graphite intercalation compounds (−2.3 kcal mol^{-1}) [5–7] and activated carbon or graphite (−0.9 to −1.25 kcal mol^{-1}) [8–11]. However, the reported hydrogen storage capacity of SWCNTs varies widely depending on the quality of the nanotubes and the pretreatment of the samples [3, 4, 12, 13]. The higher heat of adsorption in carbon nanotubes versus other graphitic materials has been attributed to the curvature of the graphene sheet when using nanotubes instead of graphite. Carbon atoms in the nanotubes adopt mixed orbital hybridizations [14] due to the structural deformation away from planar geometry and 120° C-C-C bond angles, which gives rise to acute carbon atoms of a certain extent,

M. T. Knippenberg · H. Cheng (✉)
Air Products and Chemicals, Inc,
7201 Hamilton Boulevard,
Allentown, PA 18195, USA
e-mail: chengh@airproducts.com

M. T. Knippenberg · S. J. Stuart
Department of Chemistry, Clemson University,
Clemson, SC 29634, USA

determined by the tube diameter, to interact with molecular hydrogen via a physisorption process.

Many simulations and experimental studies have attempted to determine the effective hydrogen adsorption capacity for carbon nanotubes, though none has been able to match Dillon et al.'s measured adsorption energy of −4.7 kcal mol^{-1} at the predicted loadings of 5–10 wt % H_2 at room temperature and low pressure (< 1 atm.) [3]. It was found that similar loadings can be attained at high pressures (<90 atm.) [4, 12, 13], but it is very difficult to confirm the high heats of adsorption at high loadings and low pressures. Previous simulations based on *ab initio* molecular dynamics using local density functional theory modeling the interaction of H_2 molecules in an infinite lattice of (9,9) SWCNT showed that at very small adsorption amounts (0.4 wt % H_2) the adsorption energy is substantially higher than in graphite and in graphite intercalated compounds, such as KC_{24}, CsC_{24}, etc. [15–18]. The strength of the adsorption interaction was found to largely depend on the curvature of the SWCNTs.

Several hydrogen storage system efficiency targets have been proposed in the effort to develop commercially viable hydrogen-powered fuel cell vehicles. The United States Department of Energy (DOE) has proposed a hydrogen storage system gravimetric hydrogen capacity target of 6.0 wt % hydrogen for the year 2010. To achieve this system-level target, the storage material hydrogen capacity needs to be in excess of 6 wt %. Therefore, it would be useful to model the hydrogen adsorption enthalpy at these high loadings. Molecular dynamics (MD) simulations using accurate intermolecular interaction potentials are a powerful tool to describe the highly dynamical adsorption system and to derive useful energetic information at a given temperature and a given H_2 loading in a canonical ensemble. The adsorption strength is usually characterized by an average enthalpy (heat) of adsorption, where the average is over all of the particles interacting with the surface regardless of the distances between H_2 molecules and the substrate. Unfortunately, for a finite adsorbent, such as finite SWCNT bundles, in which H_2 molecules could travel far from the adsorption sites, the energy average scheme does not necessarily reflect the essence of significant physisorption. Molecules with large distances from adsorption sites ought to be excluded in the statistical average. Furthermore, many previous simulations of H_2 storage in SWCNTs utilized nanotubes in the bundles with the same diameter [19, 20], though some simulations have been performed looking at bundles having nanotubes of different diameters [21]. In practice, SWCNT bundles are produced with non-uniform nanotube diameters. In addition to modeling tubes of the same diameter, simulations involving hydrogen adsorption have focused on infinite, periodic bundles of nanotubes. Since interstitial and endohedral adsorption sites alone do not provide a complete picture of hydrogen adsorption, a more accurate simulation would include a finite bundle of nanotubes, containing different nanotube diameters, to measure the effects of a heterogeneous distribution of nanotubes and adsorption sites on the adsorption strength. It is also unclear from previous simulations how surface effects cause the adsorption interaction at the interface of the H_2 gas phase and the SWCNT surface to differ from adsorption in bulk systems.

In a previous communication [22], we presented a simple analytical procedure to quantitatively characterize the distance dependence of physisorption strength and effective adsorption capacity for molecular physisorption in open systems and briefly illustrated the methodology using H_2 physisorption in a finite SWCNT bundle as an example. In this paper, we present detailed studies on H_2 physisorption in a variety of finite SWCNT bundles using molecular dynamics simulations with a nanotube curvature-dependent force field. The analytical procedure was utilized to analyze the distance dependency of effective adsorption energy and capacity. The main motivation of this study is summarized as follows. SWCNT has been a subject of considerable interest as a potential hydrogen storage media. We have shown in a previous MD study that only extremely small diameter nanotubes hold the promise to provide significant heats of adsorption for H_2 required to meet the DOE 2010 target [20]. The simulation was done for H_2 in homogeneous infinite SWCNT bundles. The focus of the present study is on the distance dependency of adsorption energy and effective adsorption capacity for H_2 physisorption in both finite homogeneous and heterogeneous carbon nanotube bundles of various sizes. We show that at a given H_2 loading and a given distance from the substrate the effective adsorption energy could be considerably higher than the average adsorption energy one would normally get with the effective adsorption capacity lower than the given loading. The MD simulation allows for the loading of a fixed amount of H_2 molecules into a simulation cell filled with carbon nanotubes and the subsequent movement of each H_2 molecule to be simulated over a period of time, performing a time average of structural and energetic properties.

Simulation procedure

In theory, adsorption of H_2 molecules in SWCNTs may occur not only on the outside walls of the nanotubes, but also endohedrally. This occurs in order to equilibrate the chemical potential inside and outside the nanotube [15, 23]. There are a number of possible sites for hydrogen adsorption in a bundle of carbon nanotubes. Hydrogen can adsorb on the outer wall of the carbon nanotubes on the exterior of a bundle (surface site), in the groove created by two nanotubes on the outside of the bundle (groove site), in

the pore created at the intersection of three nanotubes in the interior of the bundle (interstitial site), and inside of the nanotubes (endohedral site) (Fig. 1). The strength of adsorption is shown to be dependent upon the type of adsorption sites, with the interstitial site providing the most energetically favorable position for H_2 adsorption, due to the interaction with multiple nanotubes [21, 24].

From previous *ab initio* MD simulations dealing with hydrogen adsorption in SWCNTs [15, 16], it is clear that one of the most vital requirements for classical simulation method is the ability to account for the curvature effects of the carbon nanotubes. In addition, a reactive potential that has the ability to allow bonds to break and form would be useful in the event that chemical reactivity might be present at higher loads. Thus, the AIREBO potential [25], developed specifically for hydrocarbon interactions, will be used. This reactive potential modifies the strength of atomic interactions based on the local bonding environment as well as intermolecular interactions as well. The van der Waals interaction between hydrogen and sp^2 carbon in the original AIREBO potential was parameterized to model the interaction of hydrogen with graphite, which is a planar material. Therefore, the Lennard-Jones (LJ) interaction parameters of the AIREBO potential were modified so that they vary with the radius of curvature of the carbon nanotube as in a previously developed H_2/SWCNT potential, which provides the equations necessary for modifying the LJ parameters based on the nanotube curvature [19]. Nanotubes of different diameters can thus be simulated in the same nanotube bundle with different interaction parameters.

The physisorbed H_2 molecules may adsorb statically to a specific adsorption site, move dynamically between adsorption sites, or desorb from the surface in equilibrium with a reservoir of gaseous molecules. For most molecular simulations, the adsorption strength is defined as an average enthalpy (heat) of adsorption, where the average is calculated over all of the particles interacting with the surface. In open systems, however, this average enthalpy depends strongly on the population adsorbed, or interacting with the surface. More generally, each particle of a molecular system interacts with the surface with an interaction strength that varies with the distance of the molecule from the adsorption sites, its orientation, and the local environment.

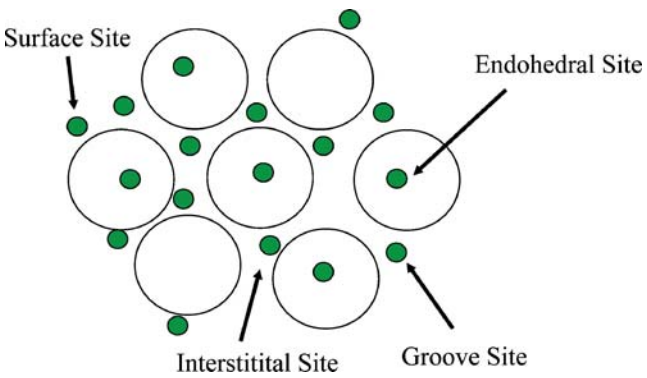

Fig. 1 Adsorption sites available in a nanotube bundle

In an attempt to precisely describe the physisorption phenomenon in an open system, we developed an analytical procedure to allow simultaneous determination of adsorption strength and effective adsorption population (i.e., surface coverage) of hydrogen in proximity to an open nanotube system where there is an interface between the nanotube surface and surrounding atmosphere containing freely moving H_2 particles [22]. Explicit distance-dependence of the average adsorption energy, as well as the effective adsorption capacity, was formulated to account for the relative interaction strength based on the distance of each H_2 molecule from the adsorbent defined by:

$$\Delta E_{\mathrm{ad}}(r) = n(r)\varepsilon_{\mathrm{gas}} + \varepsilon_{\mathrm{sub}} - \left\{\varepsilon_{\mathrm{sys}} - [N - n(r)]\left[\varepsilon_{\mathrm{gas}} + \Delta\varepsilon_{\mathrm{ads}}(r)\right]\right\} \quad (1)$$

where $\Delta E_{\mathrm{ad}}(r)$ is the average adsorption energy for all molecules within distance r of the nanotube, $n(r)$ is the number of molecules within distance r of the surface, N is the total number of H_2 molecules in the ensemble and $\varepsilon_{\mathrm{gas}}$, $\varepsilon_{\mathrm{sub}}$, and $\varepsilon_{\mathrm{sys}}$ are the average energies of a single gas-phase H_2 molecule, the SWCNT bundle, and the full system (H_2 on SWCNTs), respectively. The value $\Delta\varepsilon_{\mathrm{ads}}(r)$ is the average adsorption energy for molecules that are *outside* distance r. In essence, the adsorption energy calculated in this fashion represents the Gibbs excess heat of adsorption. A detailed description of the analytical procedure was provided in [22].

Molecular dynamics simulations were performed in a canonical ensemble using a Langevin thermostat for 50 ps at 300 K with a time step of 0.25 fs upon full structural relaxation. At the completion of the 50 ps, the energy was averaged over the last 20 ps.

Both homogeneous and heterogeneous small SWCNT bundles were chosen in the present study. The homogeneous system is composed of only (9,9) SWCNT while the heterogeneous system contains a mixture of (7,7), (9,9), and (12,12) SWCNT, which have diameters of 9.49, 12.20, and 16.27 Å, respectively. To facilitate comparison of adsorption properties between the two types of nanotube bundles, the heterogeneous nanotube bundles were made in such a way that the average diameters of the nanotubes involved in the bundles are approximately the same as the diameter of the corresponding homogeneous bundles. Each nanotube was constructed from the unit cell specific to that particular nanotube, and then replicated nine times along the nanotube axis to form a nanotube bundle.

To determine the strength of H_2 adsorption on SWCNTs, three different loadings of H_2 were used: 0.4 wt %, 3.0 wt %, and 6.5 wt %. In addition to varying the number of H_2 molecules, the number of SWCNTs can also be varied to compare the difference in adsorption strength based on the number of SWCNTs in the system. In each of the following simulations, a finite bundle of SWCNTs is created containing either three, four, or seven SWCNTs. Each bundle is centered in a box having two sides 100 Å in length, and a length of 22.14 Å along the nanotube axis, which is the length of nine unit cells of armchair SWCNTs, allowing for the simulation of infinitely long SWCNTs through the use of periodic boundary conditions. The number of H_2 molecules and their optimal endohedral and exohedral distributions, which were determined based on the lowest energy configurations, [20] in the selected SWCNT bundles are shown in Table 1. Simulations of pure nanotube bundles are performed for 50 ps with the intertube distance initially set to 3.4 Å, which represents the distance between two nanotube sidewalls in a hexagonally packed homogeneous bundle [27].

Results and discussion

During the course of each simulation at different hydrogen loads, each homogeneous bundle maintained the hexagonal packing observed for the actual SWCNT materials. For heterogeneous bundles, the intertube distance was also forced to be 3.4 Å for as many of the tube-tube contacts as possible, and the tubes placed in such a manner as to closely mimic hexagonal packing. The same overall shape found in the homogeneous bundles was maintained in the heterogeneous bundles, with the three-tube bundle packed in a triangular array and the four-tube bundle having two layers of two tubes, with the nanotube axes forming a parallelogram. The seven-tube bundle contained a center tube surrounded by six tubes. However, due to the curvature difference in each of these tubes, the heterogeneous bundles are not symmetrical like the homogeneous bundles are. The end result is similar to other heterogeneous bundles seen in [21]. An energy minimization was performed on each initial nanotube bundle to start the dynamics from the lowest energy state.

Hydrogen molecules were initially placed 2.2 Å from the surface of the nanotube sidewalls for both surface sites and endohedral sites. The distance is far enough not to induce chemisorption but close enough to allow physisorption to occur. Initial placements of surface H_2 molecules followed the surface of the nanotubes on the outside of the bundle, with the only requirement being that molecules were not close enough to one another to induce a chemical bond between H_2 molecules and the nanotube surface. Both surface sites and groove sites are filled through this manner. The interstitial sites are populated by manually placing ~ 20% of the exohedral H_2 molecules in the interstitial sites between tubes.

We first performed MD simulations on H_2 molecules in the selected nanotube bundles at various H_2 loadings and bundle thicknesses. As expected, the H_2 molecules are highly mobile in all cases. They rapidly exchange positions and move around in the bundles with time. In parallel, the nanotubes deform accordingly upon interacting with the H_2 molecules, although much more slowly. It was observed that at a low H_2 loading, H_2 molecules tend to be closer to the nanotube bundle walls; at a high loading, however, many H_2 molecules are repelled away from the nanotube

Table 1 System configurations for H_2 adsorption on finite SWCNT bundles

System	(7,7)	(9,9)	(12,12)	Wt % H_2	# H_2	# Endo H_2	# Exo H_2
3 SCWNTs (Homogeneous)	0	3	0	0.4	23	0	23
				3.0	180	72	108
				6.5	406	162	244
4 SWCNTs (Homogeneous)	0	4	0	0.4	31	0	31
				3.0	243	96	187
				6.5	540	216	324
7 SWCNTs (Homogeneous)	0	7	0	0.4	54	0	54
				3.0	423	168	255
				6.5	945	378	567
3 SWCNTs (Heterogeneous)	1	2	0	0.4	22	0	22
				3.0	167	67	100
				6.5	378	154	234
4 SWCNTs (Heterogeneous)	1	2	1	0.4	32	0	32
				3.0	247	100	147
				6.5	555	220	335
7 SWCNTs (Heterogeneous)	2	3	2	0.4	58	0	58
				3.0	450	180	270
				6.5	996	400	596

bundles due to limited adsorption sites available and H_2-H_2 repulsion. Figure 2 displays the MD maps for H_2 molecules in a 7-tube homogeneous bundle and a 7-tube inhomogeneous bundle at 6.5 wt % loading derived from the calculated MD trajectories. For clarity, the trajectory maps for C atoms are not shown here. For H_2 molecules in other nanotube bundles and at lower loadings, the calculated MD trajectory maps exhibit similar features. The H_2 molecules at the endohedral sites are incapable of penetrating the nanotube walls and thus are completely confined inside the nanotubes. Nevertheless, these molecules are not statically adsorbed near the walls. Instead, they travel in the entire space of the endohedral sites, forming layered adsorption structures, as illustrated in Fig. 2. Molecules residing in the layer close to the nanotube inner walls contribute positively to the adsorption but those in the core contribute little or even negatively to the adsorption due to the H_2-H_2 repulsion, similar to what was found for H_2 molecules in infinite SWCNT bundles [20]. At the exohedral adsorption sites, high H_2 density is observed at the interstitial and groove sites and around nanotube outer walls. A significant amount of H_2 molecules, however, travels away from the nanotube bundles. It is particularly noteworthy that in the case of heterogeneous bundle H_2 molecules are much closer to the adsorbent than in homogeneous bundle due to the fact that the heterogeneous nanotube packing opens up more surface space allowing H_2 molecules to get closer to the nanotubes.

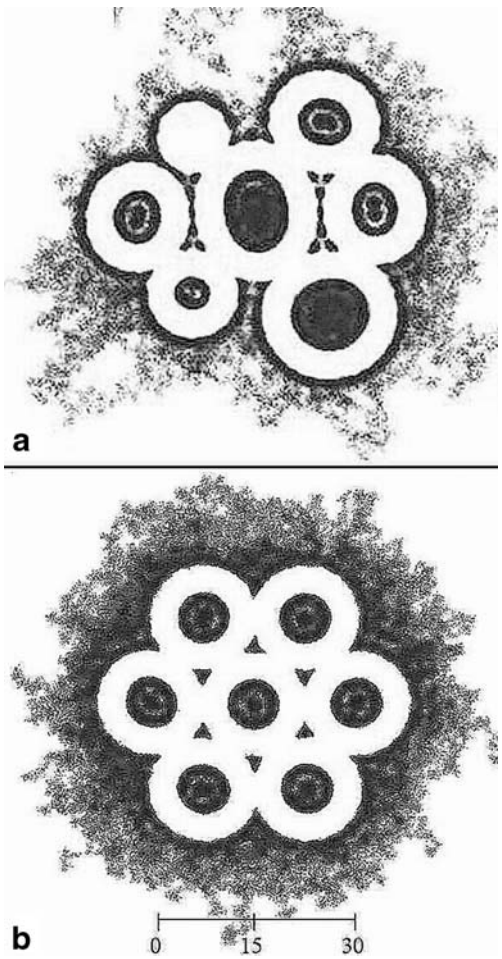

Fig. 2 The calculated MD maps for H_2 molecules in a 7-tube inhomogeneous bundle and a 7-tube homogeneous bundle at 6.5 wt.% loading derived from the calculated MD trajectories

Clearly, the adsorption strength of H_2 molecules varies, depending on the distances of these molecules from the nanotube bundles. We therefore applied the computational procedure developed previously to analyze the relative strength of adsorption as well as the effective capacity of the adsorbents and expressed these quantities in terms of H_2 distance r from the nanotube bundles [22].

Figure 3 displays the calculated H_2 radial density distribution, the effective adsorption capacity around the selected bundles, the residue energy $\varepsilon'(r)$, which denotes the average adsorption energy of all adsorbate molecules at a distance beyond r, and the average adsorption energy of H_2 molecules within the distance r at the H_2 loadings of 0.4 wt %, 3.0 wt %, and 6.5 wt % for three nanotube homogeneous (9,9) SWCNT bundle and a three-tube heterogeneous bundle. Several general features can be readily observed from Fig. 3:

1. (The majority of H_2 molecules are physisorbed within 4 Å from the nearest carbon atom, regardless of H_2 loading and nanotube bundle homogeneity, consistent with the distribution of H_2 molecules in zig-zag nanotube bundles by Huarte-Larrañaga and Albertí, which found attractive interactions to occur within 2–3 Å of the bundle surface [26]. The second layer of adsorption, formed only at the 6.5 wt % of H_2 loading, is centered around 5 Å with H_2 molecules located at both the exohedral sites and the center of nanotubes of the endohedral sites.
2. The heterogeneous radial density is very similar to the homogeneous radial density, which is expected since the only difference in bundle composition is the replacement of a (9,9) SWCNT with a (7,7) SWCNT (see Table 1) and the three heterogeneous nanotubes are close packed and thus without advantage of extra-surface area. In fact, there is even a slight decrease in the overall adsorption capacity found in the first two layers in the heterogeneous bundle, due to the decrease in surface area between the (7,7) and (9,9) SWCNTs.
3. The residue energy increases monotonically but varies only in a very narrow range in the entire space.
4. The average distance-dependent adsorption energy decreases rapidly before r=4Å and declines monotonically.
5. The average adsorption energy increases as the H_2 loading decreases.

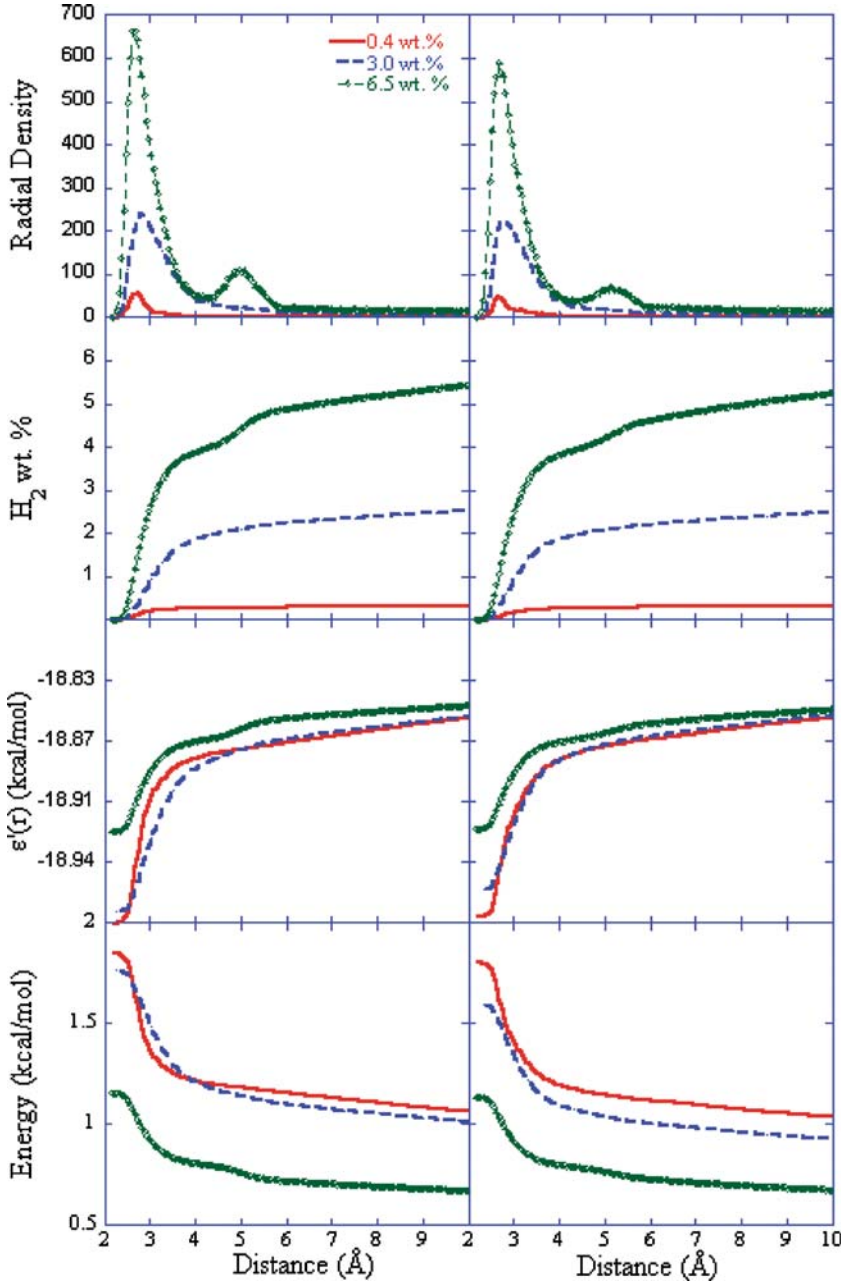

Fig. 3 Comparison of radial density, amount of H_2 found within a certain distance from the closest carbon, energy of a single H_2 molecule at distance r, and the average adsorption energy for three loadings of H_2 for both a homogeneous (left panel) and heterogeneous (right panel) three-nanotube bundle

6. Within r=4 Å, the effective H_2 adsorption capacity is slightly less than 4 wt % for 6.5 wt % H_2 loading, less than 2 wt % for 3.0 wt % loading and about 0.3 wt % for 0.4 wt % loading. The associated H_2 adsorption energies at this distance are 1.25 kcal mol^{-1} for 0.4 wt % and 3.0 wt % loadings and only 0.65 kcal mol^{-1} for 6.5 wt % loading in the case of homogeneous bundle. For the heterogeneous bundle, the values are in the same order of magnitude. Only at a distance close to r= 2 Å the calculated average adsorption energies appear to be significant. However, at this distance, the effective adsorption capacity is very small. We therefore conclude that these bundles are incapable of serving as effective H_2 storage materials.

We next examine H_2 adsorption properties in a slightly thicker nanotube bundle. Figure 4 displays the calculated results for a 4-nanotube homogeneous bundle and a 4-nanotube heterogeneous bundle at the selected three loadings. Similar features to those shown in Fig. 3 are observed. The main difference between the present case and the three nanotube bundles is that the heterogeneous bundle appears to be a slightly better adsorbent than the homogeneous one at low H_2 loadings with marginally higher

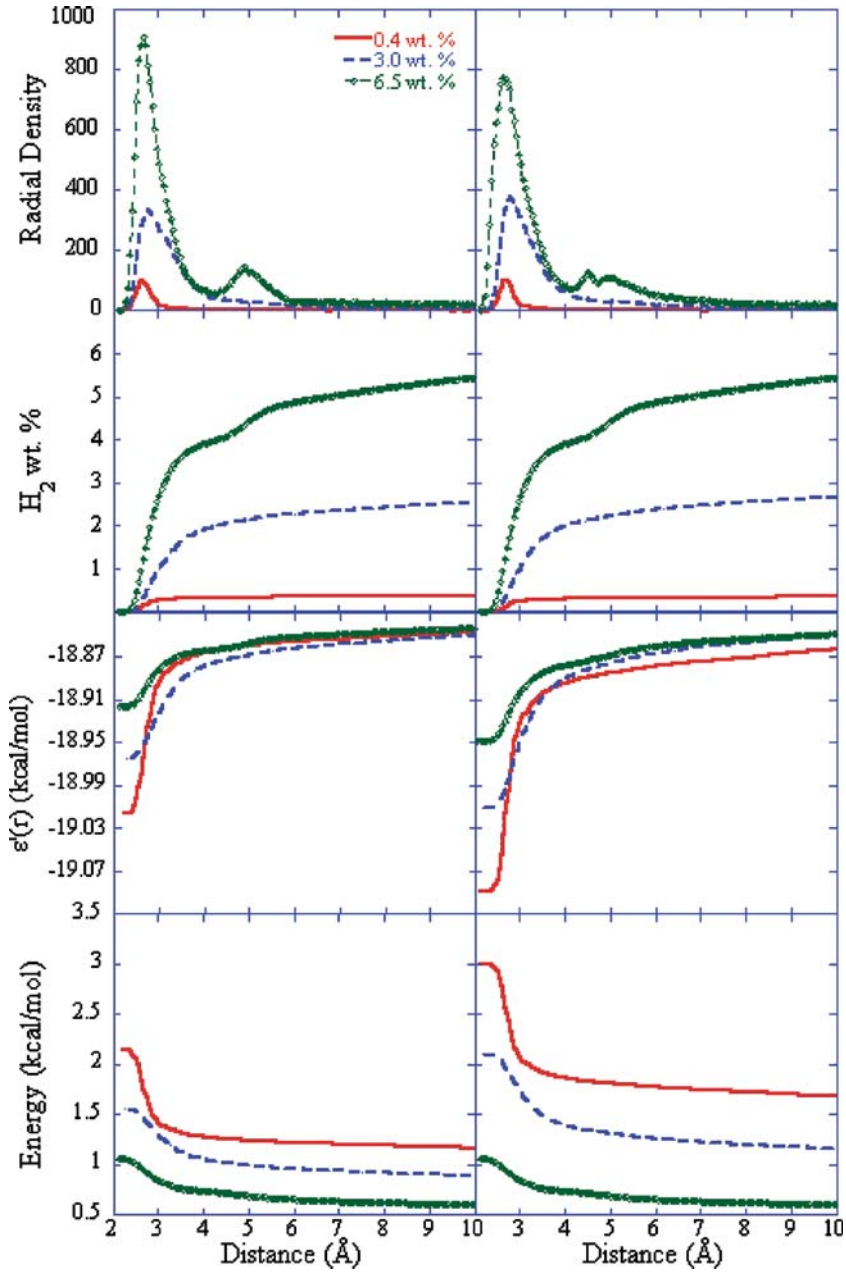

Fig. 4 Comparison of radial density, amount of H_2 found within a certain distance from the closest carbon, energy of a single H_2 molecule at distance r, and the average adsorption energy for three loadings of H_2 for both a homogeneous (left panel) and heterogeneous (right panel) four-nanotube bundle

adsorption energies. This is because the packing inhomogeneity, inherent to the 4-nanotube heterogeneous bundle, opens up more surface area in the interstitial sites for H_2 to interact with, resulting in more H_2 molecules being closer to the bundle. This result is consistent with what was reported recently by Kondratyuk, et al. using hybrid Monte Carlo simulations [28]. For 6.5 wt %, our results show that there is little difference between the homogeneous bundle and the heterogeneous bundle. Like the 3-nanotube bundles, neither of the 4-nanotube bundles is capable of adsorbing a significant amount of H_2 with an average heat of adsorption higher than 3 kcal mol^{-1}.

Figure 5 displays the calculated results for H_2 in a 7-nanotube homogeneous bundle and 7-nanotube heterogeneous bundle. The main features of the calculated properties are similar to those found for thinner nanotube bundles. However, the average adsorption energy in general becomes larger. Once again, for 0.4 wt % H_2 loading, the adsorption energy of the heterogeneous bundle is slightly larger than that of the homogeneous bundle. At higher H_2 loadings, the difference in the calculated adsorption energies of different types of nanotube bundles is marginal. Detailed numerical analysis indicates that the higher adsorption energy in the thicker

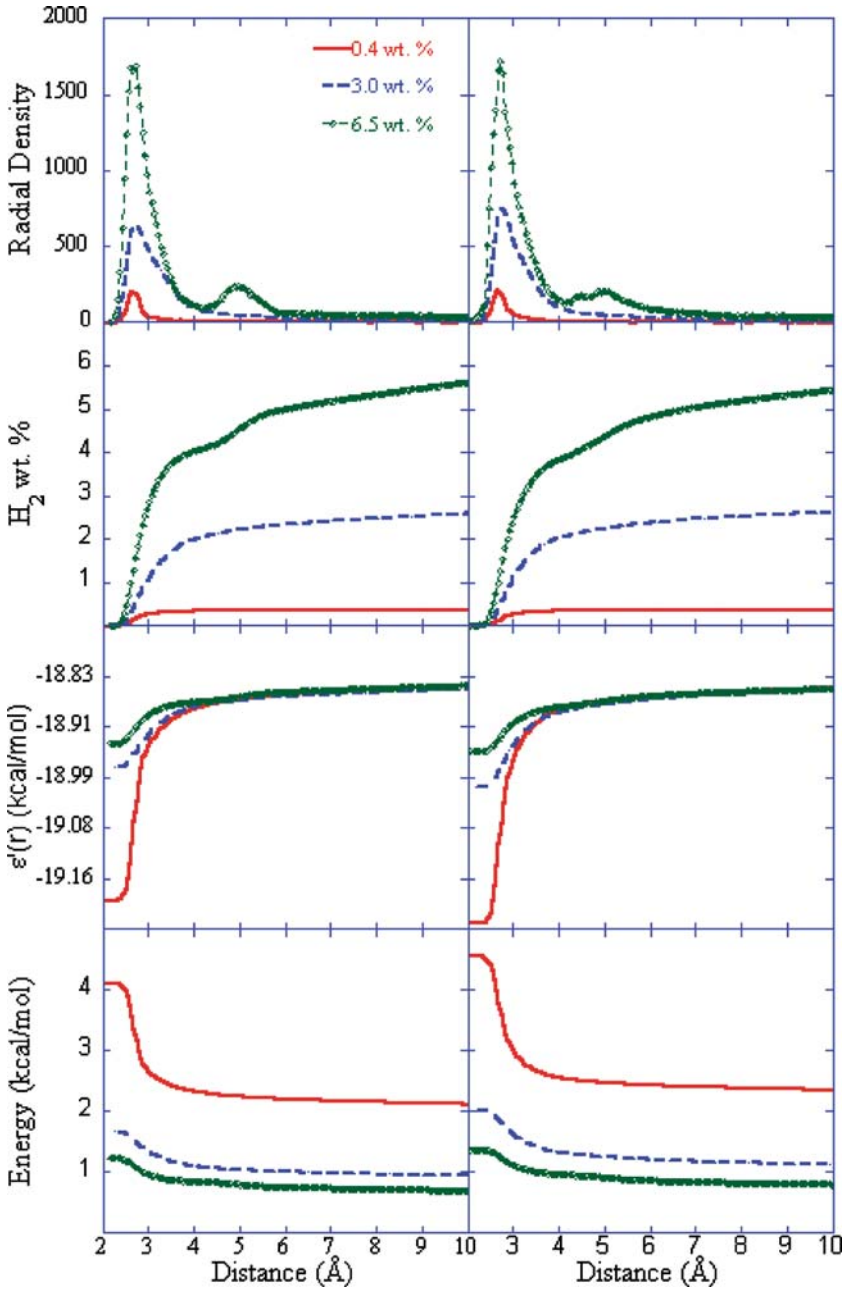

Fig. 5 Comparison of radial density, amount of H_2 found within a certain distance from the closest carbon, energy of a single H_2 molecule at distance *r*, and the average adsorption energy for three loadings of H_2 for both a homogeneous (left panel) and heterogeneous (right panel) seven-nanotube bundle

nanotube bundle arises from the slightly higher surface area of the heterogeneous bundle due to the packing inhomogeneity. In all cases, higher adsorption energy is associated with a smaller capacity value. Of the three H_2 loadings investigated in the present study, only 0.4 wt % would give an adsorption energy above 4 kcal mol^{-1} for H_2 molecules confined within 2.5 Å for the homogeneous bundle and 2.7 Å for the heterogeneous bundle. Within these distances, the effective adsorption capacity is only approximately 0.15 wt % for the homogeneous bundle and 0.35 wt % for the heterogeneous bundle. This is consistent with the experimental results reported by Shiraishi et al. [4]. For higher loadings, the calculated adsorption energies are too small for this material to be used as the storage media.

The results shown in Figs. 3, 4 and 5 indicate that in general the average adsorption energy increases with the thickness of nanotube bundles. Unfortunately, due to the computational complexity, we were unable to simulate H_2 adsorption in thicker nanotube bundles. Nevertheless, based on the results we obtained and our previous studies on infinite nanotube bundles, we conclude that further increase of nanotube bundle thickness would not result in significant enhancement of average adsorption energies.

Summary

We have performed extensive MD simulations for hydrogen physisorption in finite single walled carbon nanotube bundles to explore the possibility of using these materials as potential hydrogen storage media. The simulations were done using a curvature-dependent force field developed specifically for molecular interactions in carbon nanotubes. The effects of nanotube packing due to homogeneity and bundle thickness at several H_2 loadings on the adsorption energy and effective adsorption capacity were systematically examined. The calculated heat of adsorption and adsorption capacity were expressed explicitly in terms of average distance of H_2 from the nanotube bundle walls.

To rigorously characterize the adsorption strength, the Gibbs excess heat of adsorption should be calculated. This is not a problem for an infinite system since gap molecules are all in close interaction regimes with the adsorbent and the Gibbs excess heat of adsorption can be calculated in terms of average adsorption energy. However, for an open system, such statistical average would result in underestimation of heat of adsorption since some of the gas molecules may reside outside of the appreciable interaction regimes, i.e., far from the adsorbent. The approach developed in the present article allows one to rigorously express the adsorption energy, as well as the effective adsorption capacity, as a function of molecular distance from the adsorbent. In this case, the calculated average adsorption energy becomes the Gibbs excess heat of adsorption.

Our results indicate that the average heat of adsorption decreases rapidly with the molecular distance from the adsorbent and only a small portion of H_2 molecules is within the range that contributes significantly to the heat of adsorption. This is an important observation, because even though the gravimetric storage density of hydrogen around larger nanotubes may increase with increasing diameter [29], there is a limited surface area with which H_2 may interact, and past this point, excess H_2 molecules will have a minimal adsorption energy. In fact, our calculations show that the calculated average heat of adsorption decreases with H_2 loading, reflecting the fact that a higher loading gives rise to more repulsion among H_2 molecules. It was found that the average heat of adsorption increases slightly with the nanotube thickness but the increase is marginal for effective hydrogen storage. We also found that for a similar average nanotube diameter, H_2 adsorption in inhomogeneous bundles is slightly stronger than in homogeneous bundles because the inhomogeneous bundles provide more surface area for H_2 to interact with. Similar to what was found for infinite bundles of SWCNTs previously, we conclude that only small diameter SWCNTs hold promise for significant hydrogen storage.

Acknowledgements The authors gratefully acknowledge funding for this work provided by the U.S. Department of Energy's Office of Energy Efficiency and Renewable Energy via Hydrogen Sorption Center of Excellence.

References

1. Berry GD, Aceves SM (1998) Energy & fuels 12:49–55
2. Züttel A, Nützenadel Ch, Sudan P, Mauron Ph, Emmenegger Ch, Rentsch S, Schlapbach L, Weidenkaff A, Kiyobayashi T (2002) J Alloys and Compounds 330:676–682
3. Dillon AC, Jones KM, Bekkedahl TA, Kiang CH, Bethune DS, Heben MJ (1997) Nature 386:377–379
4. Shiraishi M, Takenobu T, Ata M (2003) Chem Phys Lett 367:633–636
5. Watanabe M, Soma M, Onishi T, Tamaru K (1971) Nat Phys Sci 233:160–161
6. Watanabe K, Kondow T, Soma M, Onishi T, Tamaru K (1973) Proc Roy Soc Lond A A333:51–67
7. Terai T, Takahashi Y (1989) Synth Met 34:329–334
8. Pace EL, Siebert AR (1959) J Phys Chem 63:1398–1400
9. Dericbourg J (1976) Surf Sci 59:565–574
10. Constabaris G, Sams Jr JR, Halsey Jr GD (1961) J Phys Chem 65:367–369
11. Benard P, Chahine R (2001) Langmuir 17:1950–1955
12. Liu CY, Fan Y, Liu M, Cong HT, Cheng HM, Dresselhaus MS (1999) Science 286:1127–1129
13. Ye Y, Ahn CC, Witham C, Fultz B, Liu J, Rinzler AG, Colbert D, Smith KA, Smalley RE (1999) Appl Phys Lett 74:2307–2309
14. Okamoto Y, Miyamoto Y (2001) J Phys Chem B 105:3470–3474
15. Cheng H, Pez GP, Cooper AC (2001) J Am Chem Soc 123:5845–5846
16. Canto G, Ordejón P, Cheng H, Cooper AC, Pez GP (2003) New J Phys 5:124.1–124.8
17. Cheng H-M, Yang Q-H, Liu C (2001) Carbon 39:1447–1454
18. Simonyan VV, Johnson JK (2002) J Alloys and Comp 330:659–665
19. Kostov MK, Cheng H, Cooper AC, Pez GP (2002) Phys Rev Lett 89:146105.1–146105.4
20. Cheng H, Cooper AC, Pez GP, Kostov MK, Piotrowski P, Stuart SJ (2005) J Phys Chem B 109:3780–3786
21. Shi W, Johnson JK (2003) Phys Rev Lett 2003 91:015504.1–015504.4
22. Knippenberg MT, Stuart SJ, Cooper AC, Pez GP, Cheng H (2006) J Phys Chem B 110:22957–22960
23. Yang FH, Lachawiec Jr AJ, Yang RT (2006) J Phys Chem B 110:6236–6244
24. Dresselhaus MS, Williams KA, Eklund PC (1999) MRS Bull 24:45–50
25. Stuart SJ, Tutein AB, Harrison JA (2000) J Chem Phys 112:6472–6486
26. Huarte-Larrañaga F, Albertí M (2007) Chem Phys Lett 445:227–232
27. Salvetat J-P, Briggs GAD, Bonard J-M, Bacsa RR, Kulik AJ, Stöckli T, Burnham N, László F (1999) Phys Rev Lett 82:944–947
28. Kondratyuk P, Wang Y, Johnson JK, Yates Jr JT (2005) J Phys Chem B 109:20999–21005
29. Weng C-I, Ju S-P, Fang K-C, Chang F-P (2007) Comp Mater Sci 40:300–308